

Core Data and the MRIL* Show A New Approach To " Formation Factor "

G. R. Coates, A. D. Howard, Numar Corporation

Abstract:

A new wireline logging technology, the Magnetic Resonance Imaging Log (MRIL*), is now available to the industry. The basic concepts, ^{1,2,3}the tool's measurements and the comparison of the MRIL, in select environments, to core data and other logs have previously been published. However, the wealth of information that this tool brings opens the way to changing many of the ways formation evaluation is done. This paper reports on one of these, a study which links the MRIL to a key petrophysical property, water saturation.

By using comparison to both core and conventional log data, it is shown how the MRIL measurement can be used to improve log derived water saturation values. This is accomplished by establishing a tie between the MRIL and an exponent relating the bulk-volume water (BVW) content and the formations resistivity properties.

As many other industry reports have shown⁴, the bulk resistivity of the formation is responding to the BVW and its conductivity. These properties are traditionally related through the Archie functions where the BVW is separated into two individual components, the porosity and the water saturation, each then being exponentially related to formation factor and saturation respectively.

Another option, also already in the literature⁵, relates the BVW to the rocks R_w/R_t ratio through use of a single exponent, w . This paper reports on an investigation of the opportunity presented by the MRIL to determine w using the measured bulk volume of irreducible water (MBVI), as well as the total porosity (MPHI), in hopes of improving log derived saturation results. Core based values of m and n are also converted to w for verification purposes. From this set of information a technique is proposed for refining the saturation determination process, as well as revealing a new way to examine a zone's irreducible saturation qualities.

Anyone dealing with saturation determination from well logs, especially in complex lithologies, should find these approaches useful.

Introduction:

In log interpretation, the standard approach to water saturation is through the Archie⁶ formation factor (FF) process. Application of this approach depends on an analyst selecting some link between FF and porosity. In most cases the analyst will use the same relationship over large intervals, intervals that may include a variety of lithologies, pore types, and grain sizes. The question often asked is, " what is the right value of a , m , and n to use?". A significant concern since these parameters are used to relate porosity to FF, and, in conjunction with resistivity, to saturation.

* Registered Trademark of NUMAR

The exponential relationships used in this process, as log analysts know, describes a link between resistivity and saturation as if the response was independently linked to porosity and saturation. This has been a useful model when doing laboratory studies, but, in consideration for how the resistivity log sees the rock, unnecessary. To a resistivity, or conductivity, log the controlling factors are the volume of fluids and their conductivity. As such it means that a slightly different approach can be taken, one that eliminates porosity and saturation as independent variables and uses only the bulk volume water term (the product of porosity and saturation) to model the relationship between conductivity of the fluids involved and the measured conductivity of the formation.

Although this approach is not new⁵, the availability of a direct measure of the volume of irreducible water (BVI), as provided by the MRIL, brings a new opportunity, one that may help log derived water saturations to be determined more reliably, especially in complex lithologies.

Relationships:

The proposed single exponent expression used to relate bulk-volume water to resistivity is;

$$(\text{PHI} * \text{Sw})^w = \text{Rw}' / \text{Rt}$$

where:

w is the exponent used to relate the BVW to Rw/Rt

PHI is the rocks total porosity

Rw' is the resistivity of the formation water including an accounting for clay water effects and,

Rt is the rocks true resistivity.

Previously, the log analyst could only assume a rock to be water filled in order to examine the apparent w value. This was, of course, only valid in the water zones and resulted in an overestimation of w in the hydrocarbon zones of interest. This problem is overcome with the availability of BVI from the MRIL. Now the analyst can solve for a second apparent w, one that is meaningful in the hydrocarbon zones. Determining both apparent w's, (ww for Sw=1.0 and wi for Sw=Sirr), brings other benefits, such as a quick look irreducible saturation profile based on the interplay between a modeled relationship for w and the two apparent values for one.

It is also possible to relate core determined m and n data to the single exponent core w using;

$$\text{Core } w = (m(\log \phi) + n(\log \text{Sirr})) / (\log (\phi \times \text{Sirr}))$$

This permits the comparison of log predicted w values from the proposed technique to core measured values.

Example 1:

This Texas Miocene example, fig S1, typifies the high porosity shaly sands of the Gulf Coast area where logs often find a hydrocarbon show even though it's not always evident that they are meaningful, since they can be the result of the analyst's sensitive parameter selections. The analyst's choice of a, m, and n, in the Archie based methods is a good example of this problem.

In this example, the bulk-volume water shown in track 4 of fig S8 is derived using a conventional Dual Water saturation⁷ model where $a=1$, $m=1.8$, $n=2$, and, as the display illustrates, there are some shows of hydrocarbon in these sands. The use of MRIL BVI seems to illustrate that most of these water saturations are non-irreducible, the exception apparently being the very upper portion of the upper sand.

Another key parameter to be selected in this process is R_w . The Pickett plot, a log-log plot of resistivity and porosity, has been found useful in such formations since the literature gives us confidence in selecting which porosity formation factor response to use. Such a plot is shown in fig S2 for the interval shown. In addition, the highest porosity, highest saturation points have been isolated and depth located on the adjacent display of MRIL data to illustrate the source of the observed trend that gives $R_w = .03$ ohmm. A small cluster of points below this trend line are also noted which are associated with a matrix lithology change, possibly an increase in calcite cement since porosity decreases and density-sonic separate (see fig S1).

With R_w selected for the clean sands, and knowing the clay water conductivity (C_{cw}) as a function of formation temperature⁷, it is only necessary to determine the fraction of the porosity (S_{wb}) containing the ionic held, clay mineral associated, water to determine the equivalent formation water conductivity. This has been done using a multiple clay indicator sorting to determine the appropriate clay bound water fraction. From this information we are able to derive a corrected C_w' , i.e.;

$$\text{where; } C_w' = C_w + S_{wb}(C_{cw} - C_w)$$

$$\text{and, } C_w = 1 / R_w$$

Determining w_w and w_i :

This brings us to the real objective of this paper, determining the exponential relationship between the bulk volume water of the formation and the resistivity ratio R_w'/R_t . This is approached by examining the apparent value of this exponent, w , by making two assumptions, a) the zones are at irreducible ($S_w = S_{irr}$, $w = w_i$), or b) that they are water filled ($S_w=1.0$, $w = w_w$).

$$w_i = \log(R_w'/R_t) / \log(MBVI)$$

$$w_w = \log(R_w'/R_t) / \log(\Phi)$$

where R_w' reflects the clay correction

The results of this are shown in track 3 of fig S3. We note first that the two estimates of w tend to approach similar values when MPHI approaches MBVI, and diverge as MPHI diverges

from MBVI. The absolute values are also worth noting, w_w ranges between 1.6 and 3.6 while w_i varies between .5 and 2.4.

Displaying w_w and w_i against R_{xo}/R_t , fig S4 and fig S5 respectively, provides a comparison of these apparent values of w against a variable strongly linked to saturation⁸, but one that is largely free of formation factor influence. This provides some additional insight into w characteristics.

Looking first at the w_w plot, several circumstances are identifiable, sands at irreducible, sands approaching $S_w = 1$, shaly sections, a mineral change and trends reflecting the effects of clay minerals and hydrocarbon content. In water sands, at or near the assumed condition, w approaches a value of 1.8, a value often observed in lab studies of similar rocks.

Looking next at the w_i plot illustrates the changes in data patterns associated with the change in assumption. Now the sands that are high in hydrocarbon content give values more in line with traditional m values, while the non-irreducible are giving values much lower. Of particular importance is the observation that w apparently varies with irreducible water saturation, meaning the traditional use of constant values in both water and hydrocarbon zones may lead to error. If the trend shown is typical, it infers that we've been over estimating hydrocarbon content using traditional m and n values in some formations while underestimating them in others. This is further examined in fig S6, a plot of w_i against w_w , where it's observed that water bearing sands are a vertical trend at a value near 1.8 while the sands at S_{irr} trend to the right and above this same value.

Another way to examine this behavior is shown in fig S7 where w_w is plotted against the apparent S_{irr} determined from the MRIL ($S_{irr} = MBVI/MPHI$). Here it is possible to readily discern trends associated with the effects of increasing S_w as well as trends of increasing S_{irr} . A trend between S_{irr} and w is also shown, providing the pattern needed for developing a relationship for predicting the value to use in a shaly sand formation like these.

The impact of using w determined in this manner, i.e.;

$$w = .4 * S_{w_{irr}} + 1.65$$

on the resulting bulk-volume water is shown in fig S8.

Here the results have increased the water in the original "shows" while reducing it in others. This figure also illustrates the capability of the w information to predict S_{irr} qualities by comparing the predicted w to w_w and w_i . When $w_w > w$ hydrocarbon are present, and when w is greater than w_i indicates non- S_{irr} , only when $w = w_i$ can the zone be considered at S_{irr} .

The show at the top of the upper sand, fig S8, was production tested, making 600 mcfpd of gas for 30 days then it started to produce about 20 BWPd and 50 BOPD, finally leveling off at 40 BOPD and 100 BWPd.

Example 2:

This example, in a more complex carbonate formation, as illustrated by the log data in fig C1, follows an investigation similar to example 1. The interval shown is an Edward's formation from central Texas. As shown by the conventional porosity logs, (see track 3) displayed in apparent limestone porosity units, the lithology is complex and finding comfort with values for a , m , and n is difficult. The core derived porosity is shown in track 4 where the MRIL log demonstrates its capability to determine porosity without concern for matrix lithology. This minimizes the porosity issue but still leaves the issue of relating it to formation factor.

Because of this good match of MRIL porosity to core, we've chosen to use it in this study. The first pass analog results of w_i and w_w are shown in fig C1. The w_w plot of this interval is shown in fig C3. The R_{xo}/R_t maximum gives good confirmation of the R_{mf}/R_w ratio and recognition that a major portion of this interval has a high water content. Looking next at the MBVI based w_i plot, fig C4, we find confirmation of the high water content as well as evidence that there are hydrocarbons present. This is indicated by the contrast in w_i and w_w . These conclusions are also supported on fig C5, a plot of w_i against w_w .

The comparison of w_w to the MRIL's predicted S_{irr} is shown in fig C6. The trend observed in the shaly sand example is shown, closely agreeing with the lower edge of the data. The data that falls above this line infers non-reservoir rock at S_{irr} or hydrocarbon effects.

Core w Determination:

Table 1 shows the results of full core analysis on similar rocks from a nearby well in this field. The results of transforming the conventional a , m , and n into w are also listed. Fig C7 shows a plot of this derived w against core S_{irr} along with a line representing the trends observed on both the shaly sand and the log derived values shown in fig C6. Though the data set is limited, it gives a fairly reasonable agreement to the observed trend.

Applying this algorithm results in the answers shown in fig C8 where the w to be used is first calculated then constrained to be greater than or equal to w_i and less than or equal to w_w . The results are quite interesting, showing that most of the good permeability section is in a non- S_{irr} state. The production tests on this well confirmed this by initially producing a 1.1 MMCF gas with low water flow from all major porosities in this interval, however, that quickly changed to non-commercial high water cut production in less than 60 days.

Conclusions:

The evidence has shown;

- a) that a , m , and n are not needed and that a single exponent, w , is adequate to relate the water volume to resistivity.
- b) that this exponential relationship between water volume and resistivity is dependent on the saturation properties.
- c) that having a direct measure of bulk volume of irreducible water not only is useful to the determination of perm^9 and the detection of irreducible conditions but also to understanding the actual volume of water suggested by resistivity logs.

References;

- 1) Miller, M., et al; " Spin Echo Magnetic Resonance Logging: Porosity and Free Fluid Determination", SPE 20516, Oct. 1990
- 2) Coates, G., et al; " The MRIL in Conoco 33-1, An investigation of a new Magnetic Resonance Imaging Log", 1991 SPWLA Trans.
- 3) Coates, G., et al; " The Magnetic Resonance Imaging Log Characterized with Petrophysical Properties and Laboratory Core Data", SPE 22723, Oct. 1991.
- 4) Worthington, P.F., "The Evolution of Shaly Sand Concepts in Reservoir Evaluation", The Log Analyst, Jan.-Feb. 1985.
- 5) Coates, G., et al; " A New Approach to Improved Log Derived Permeability", 1973 SPWLA Trans.
- 6) Archie, G., " The electrical resistivity as an aid in determining some reservoir characteristics", 1942 AIMM Engineers Trans.
- 7) Clavier, C., et al; " The Theoretical and Experimental Bases for the Dual Water Model for the Interpretation of Shaly Sands", Journal of Petroleum Technology, April 1984.
- 8) Dumanoir, J., et al., " R_{XO}/R_t Methods for Wellsite Interpretation," The Log Analysts, Vol. XIII, 1972
- 9) Timur, A., " An Investigation of Permeability, Porosity, and Residual Water Saturation Relationship", 1968 SPWLA Transactions.

Table 1
Core values in Edward's Carbonate, Central Texas.

Depth	m	n	w	PHI	PERM	SAT
10380.80	1.888	1.230	1.802	12.800	1.200	73.500
10382.60	2.063	1.020	1.738	6.300	.510	28.600
10383.60	2.021	1.020	1.823	6.700	.130	51.300
10451.40	2.119	1.120	1.796	9.200	.910	32.00
10452.80	2.111	1.230	1.758	9.700	2.500	21.00
10453.40	2.055	1.160	1.688	11.200	5.500	21.900

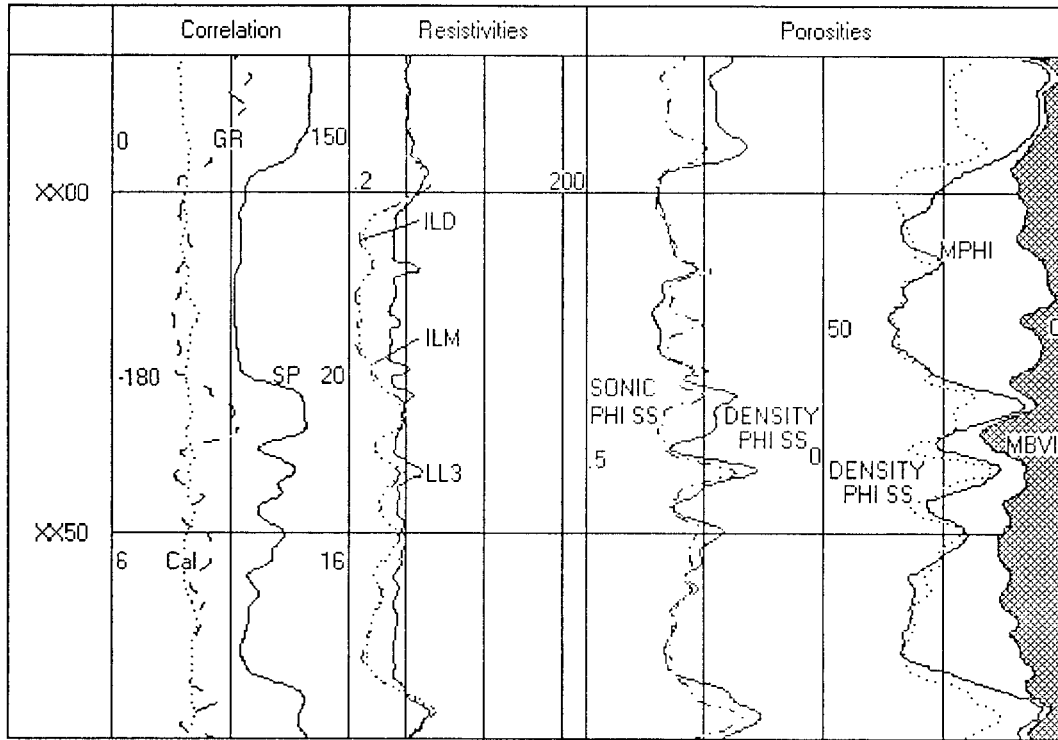


Fig S1 - Conventional logs with MRIL in Texas Coastal Miocene Formation.

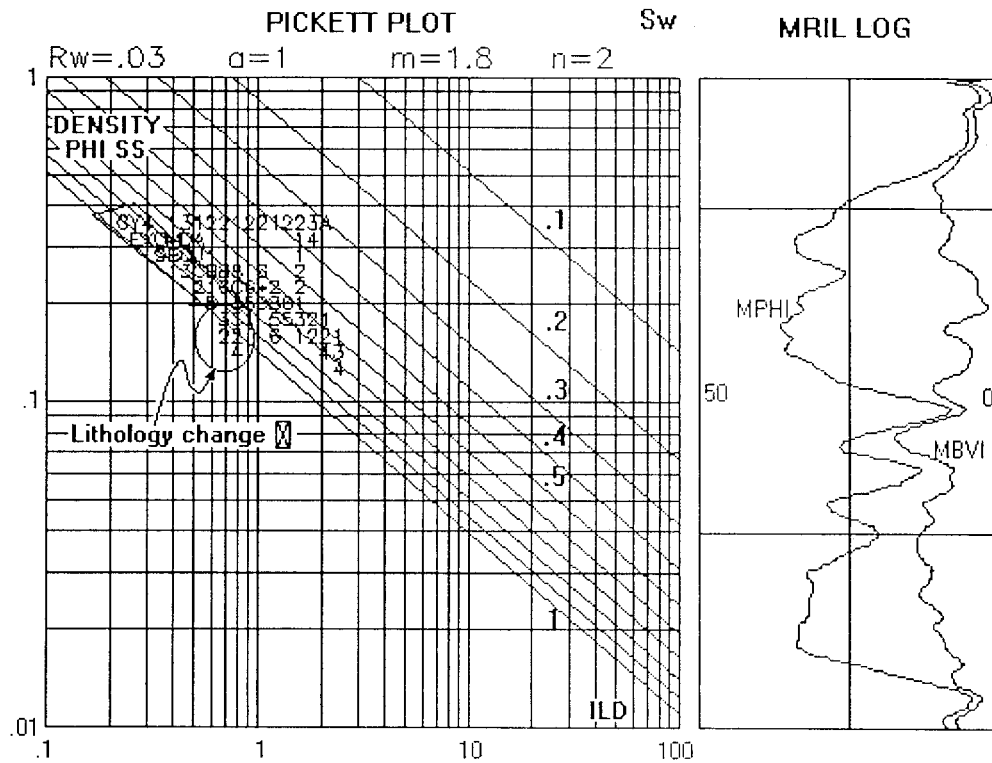


Fig S2 - Pickett Plot showing water trend used to select R_w and interval contributing to this group.

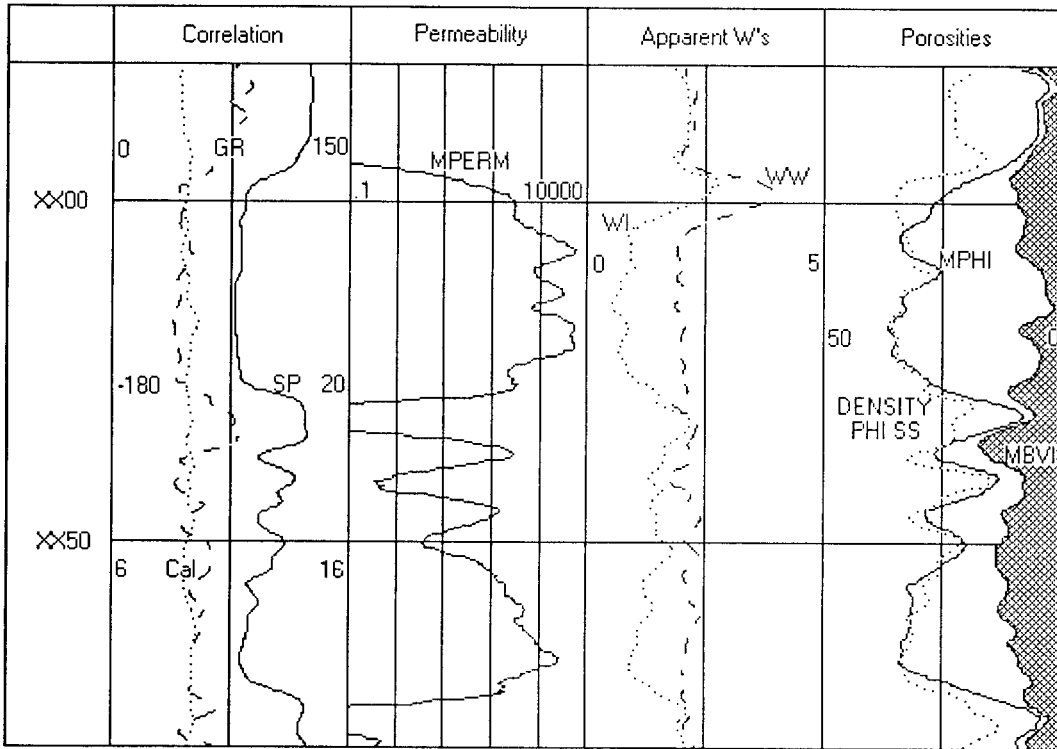


Fig S3 - Analog display of apparent "w" values in contrast to MRIL porosity and permeability.

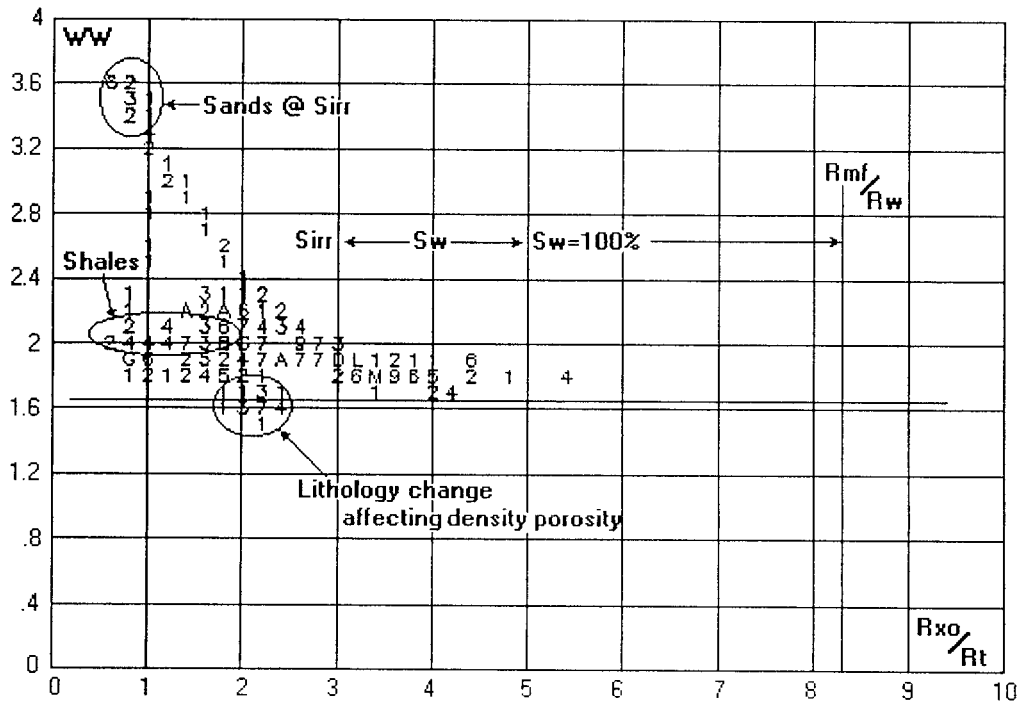


Fig S4 - Comparison of the apparent "w" values, assuming Sw=1.0 against Rxo/Rt index.

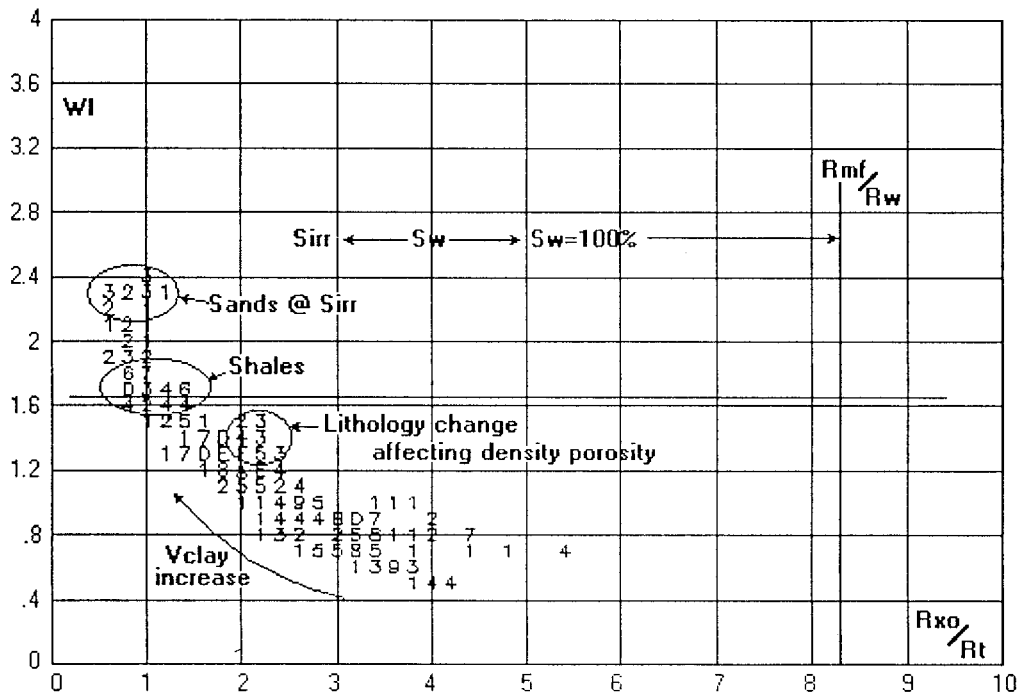


Fig S5 - Comparison of the apparent "w" values, assuming $S_w = S_{irr}$, against R_{xo}/R_t index.

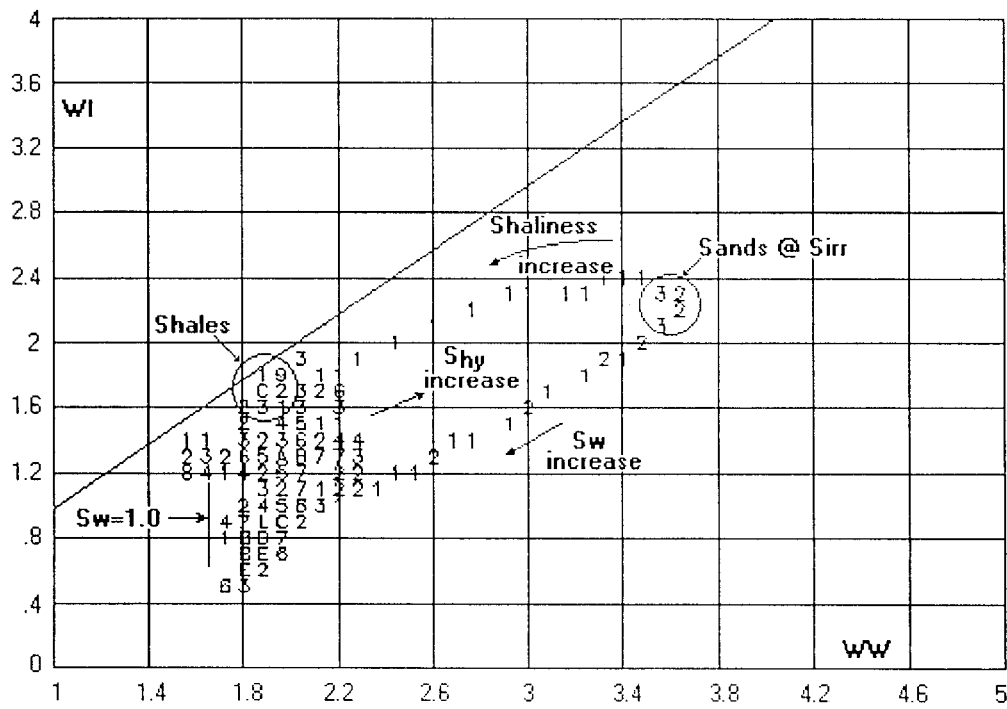


Fig S6 - Comparison of the two apparent values for the end-point conditions $S_w = 1$ and $S_w = S_{irr}$, exhibiting relative effects of S_w change.

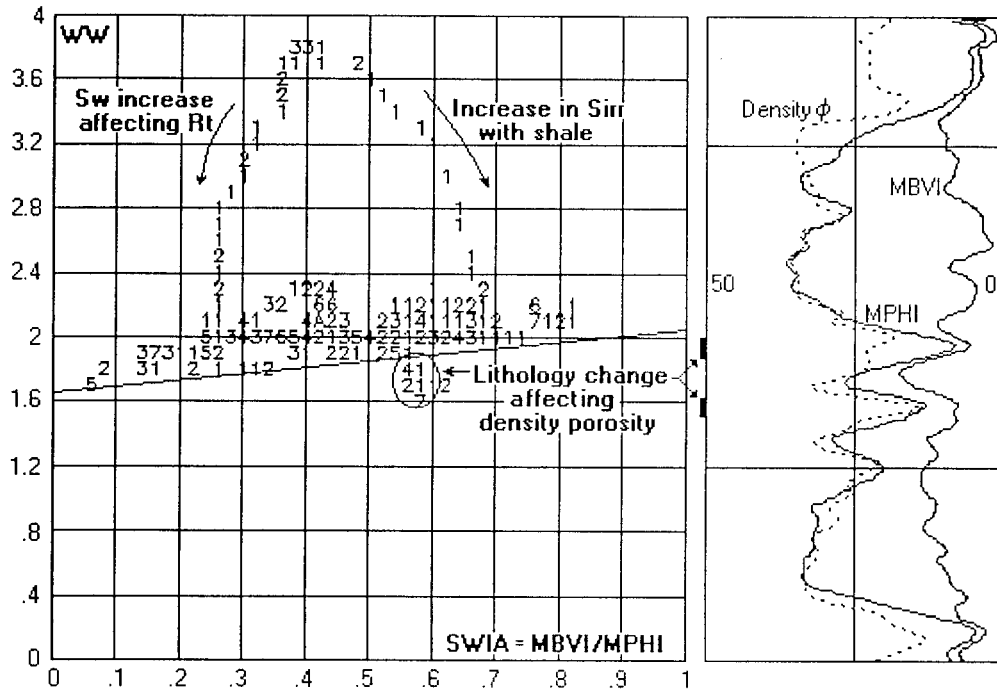


Fig S7 - Comparison of apparent value of "w", assuming Sw=100%, against apparent Sirr from MRIL.

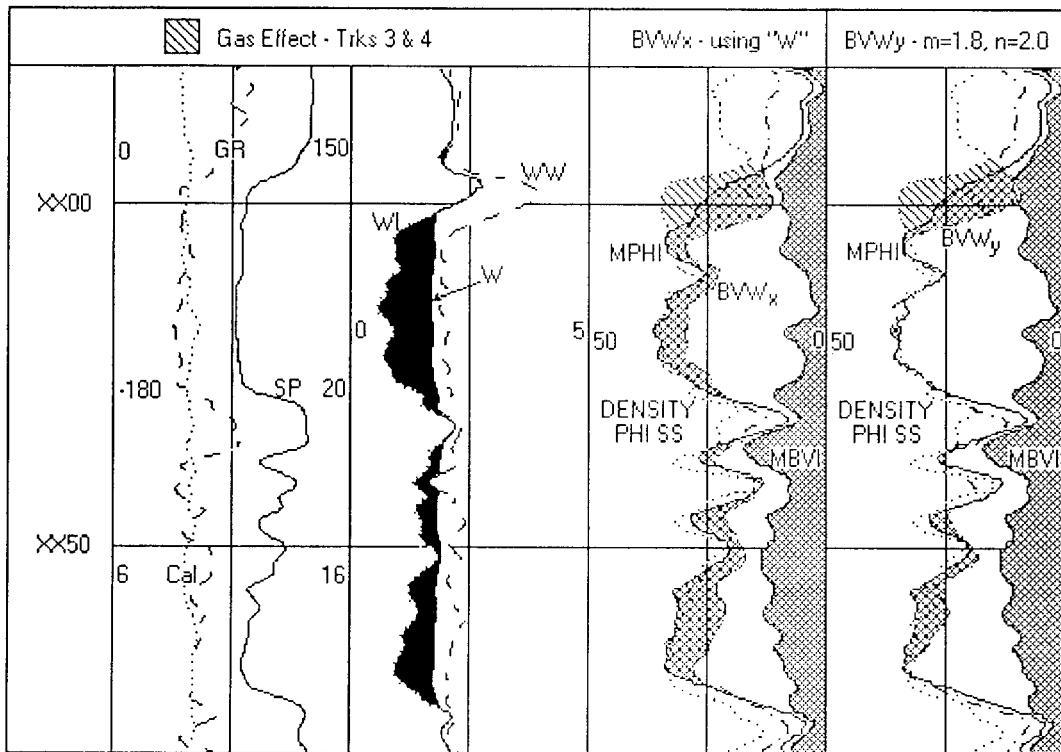


Fig S8 - Comparison of conventional results (Trk 4) with results using "w" approach, all other parameters held equal.

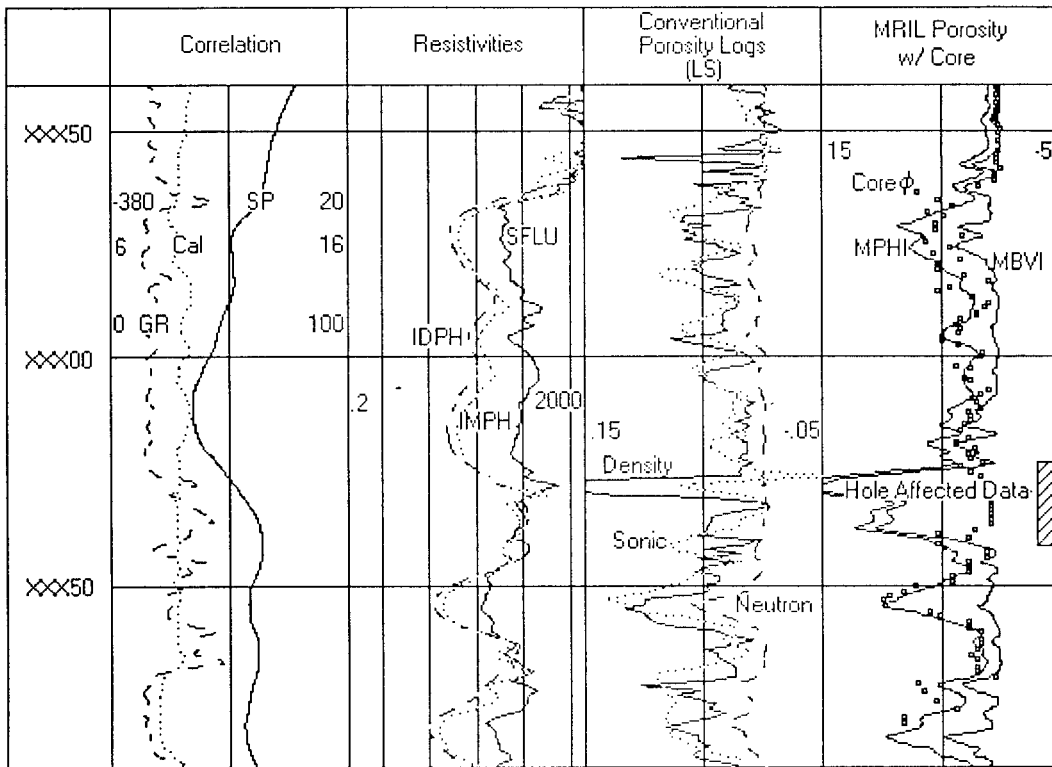


Fig C1 - Conventional Logs with MRIL in Edward's Formation.

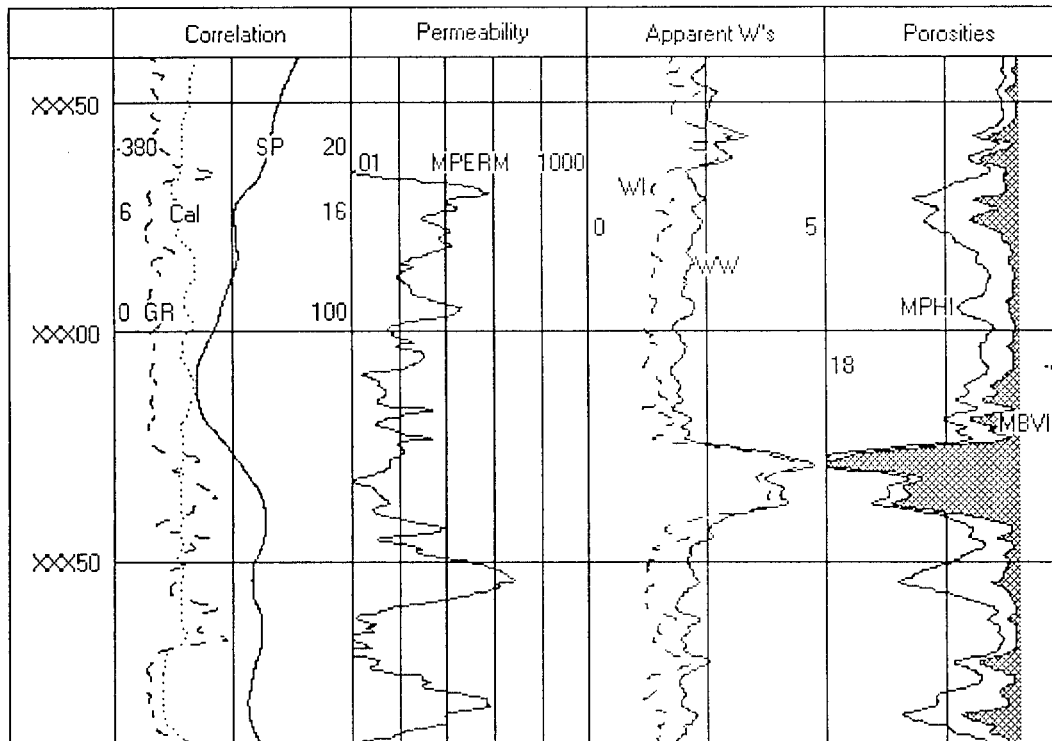


Fig C2 - MRIL data with apparent "w" values.

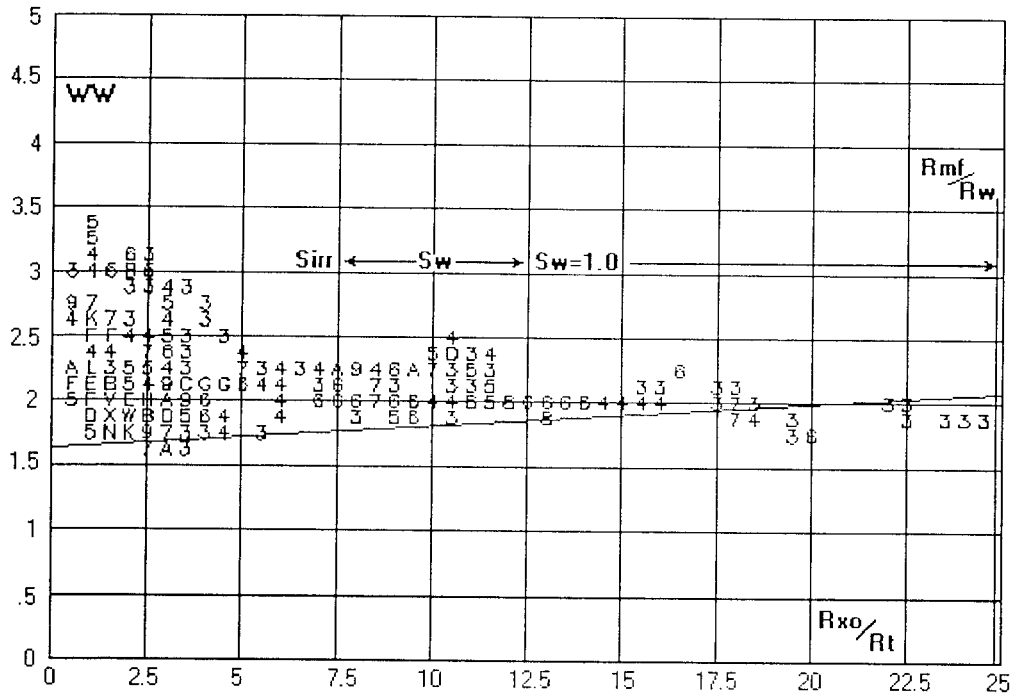


Fig C3 - Comparison of Rxo/Rt to the apparent "w" assuming Sw=1.

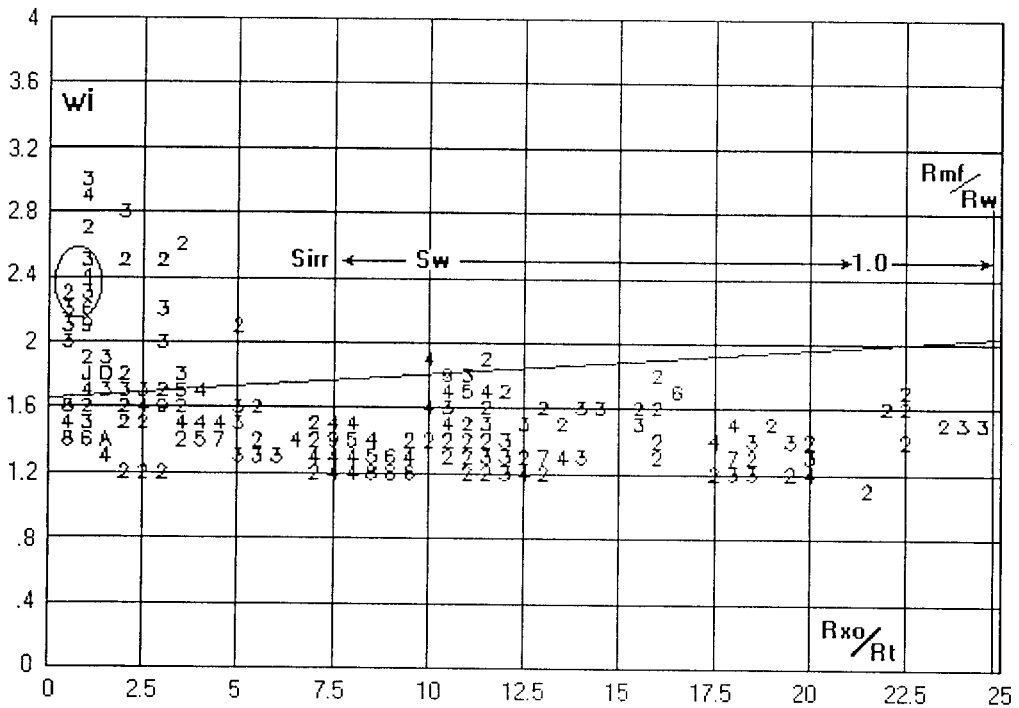


Fig C4 - Comparison of Rxo/Rt to "w" apparent assuming Sirr.

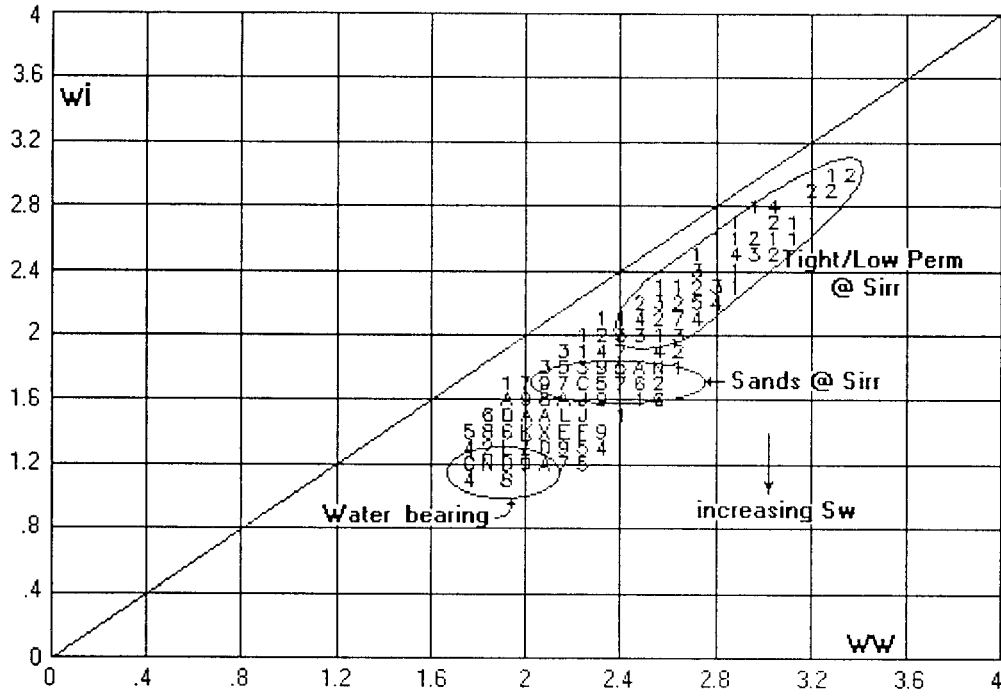


Fig C5 - "wi - ww" comparison in Edward's carbonate.

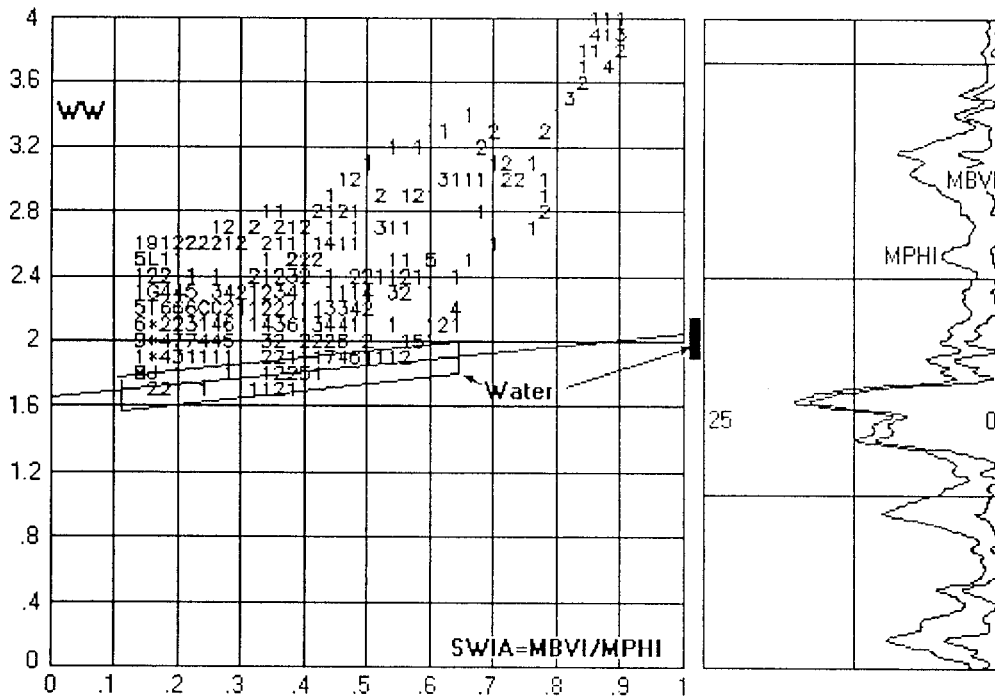


Fig C6 - Comparison of MRIL Sirr to apparent "w" assuming Sw=1.0.

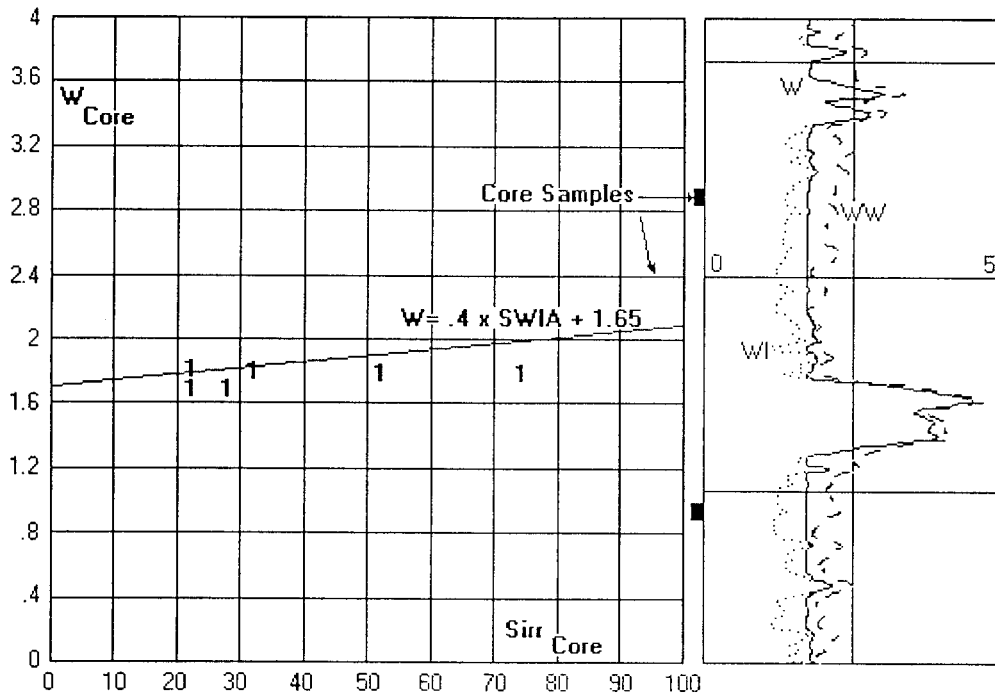


Fig C7 - Comparison of core determined Sirr and "w" parameters.

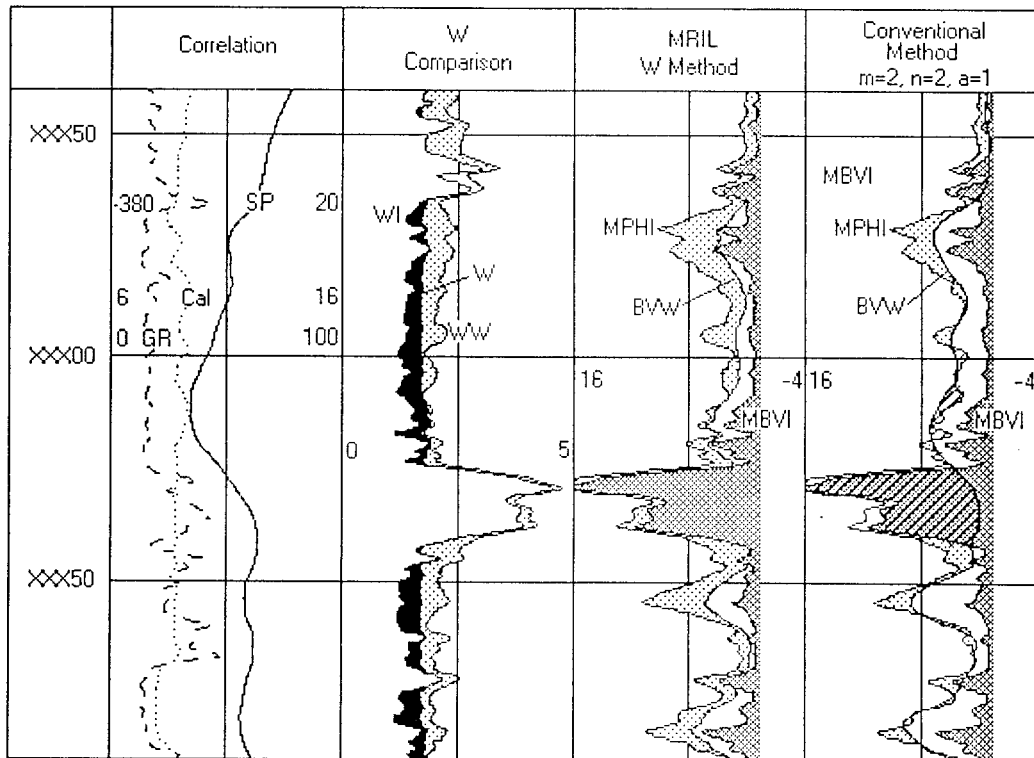


Fig C8 - Comparison of bulk volume answers with "w" and with conventional methods.